New physics in LHC Higgs boson pair production

Matthew J. Dolan,[*] Christoph Englert,[†] and Michael Spannowsky[‡]

Department of Physics, Institute for Particle Physics Phenomenology, Durham University,
Durham DH1 3LE, United Kingdom

Multi-Higgs production provides a phenomenologically clear window to the electroweak symmetry-breaking sector. We perform a comprehensive and comparative analysis of new electroweak physics effects in di-Higgs and di-Higgs + jet production. In particular, we discuss resonant di-Higgs phenomenology, which arises in the Higgs portal model and in the minimal supersymmetric Standard Model at small $\tan \beta$, and nonresonant new-physics contributions to di-Higgs production in models where the newly discovered Higgs candidate is interpreted as a pseudo-Nambu-Goldstone boson. We show that, for all these scenarios, a measurement of the di-Higgs and di-Higgs + jet final states provides an accessible and elaborate handle to understand electroweak symmetry breaking in great detail.

I. INTRODUCTION

Both ATLAS and CMS have observed a Standard Model (SM)-like Higgs boson [1] at around 125 GeV [2,3]. In the very same mass region, the combination of the DØ and CDF collaborations' data sets exhibits an SM-like Higgs excess with a local significance of 2.2σ [4]. The implications of this newly discovered particle have already been discussed in the context of the SM and beyond [5–7]. The combined local significance is mostly driven by an excess in the diphoton invariant mass, consistent with the SM Higgs boson within 2σ. Therefore, we can expect that the observed particle bears some resemblance to the SM Higgs since $gg \rightarrow h \rightarrow \gamma\gamma$ is sensitive to the special role of the Higgs particle in both the SM's gauge and Yukawa sectors and their interplay. Correlating this observation with electroweak precision data [8] and measurements in the $h \rightarrow ZZ$, W^+W^- channels, which constrain the particle's couplings to massive gauge bosons, we infer from fits to the data [5,6] (most notably by ATLAS themselves [9]) that the particle reproduces SM Higgs properties within $1–2\sigma$. This agreement partially relies on biasing the fit towards the SM Higgs hypothesis by assuming a total decay width $\Gamma(h \rightarrow \text{anything}) \simeq \Gamma_h^{\text{SM}}$ [9] and the absence of new degrees of freedom in gg, $\gamma\gamma \rightarrow h$. These assumptions are, strictly speaking, neither theoretically nor experimentally motivated. A precise determination of the particle's couplings relaxing such assumptions is an LHC lifetime achievement, which will combine direct searches for heavy states that potentially run in production and decay loops and constraints of nonstandard Higgs branching fractions.

Deviations from the SM Higgs phenomenology even at the 10% level leave a lot of space for modifications of the Higgs sector by beyond-the-SM (BSM) physics; new physics of roughly that size is largely unconstrained by the precise investigations of the SM at the Z mass pole. Given that the corresponding BSM couplings need to be small, the current data does not provide constraints on weakly coupled Higgs-sector extensions beyond what we have already learned from LEP [8]. Currently, Monte Carlo-based analyses which target nonstandard decays of the Higgs-like resonances [10–14] suggest that branching-ratio limits of $\lesssim \mathcal{O}(10\%)$ can in principle be obtained at the LHC from direct measurements, depending on the characteristics of the nonstandard decay. This bound might be too loose to efficiently probe interactions beyond the SM.

From this perspective, it is imperative to directly probe potential modifications of the electroweak symmetry-breaking sector, if phenomenologically possible, to fully exhaust the LHC's search potential to physics beyond the SM. One class of hadron collider processes which precisely serve this purpose is multi-Higgs production [15]. These processes are functions of the symmetry-breaking potential's parameters and are, consequently, highly sensitive to the realization of electroweak symmetry breaking. While triple Higgs production is beyond the reach of the LHC experiments [16], di-Higgs production can potentially be measured in rare decays $pp \rightarrow hh \rightarrow b\bar{b}\gamma\gamma$ [17]. Only recently, the application of jet substructure techniques [18] to di-Higgs production in boosted final states has uncovered sensitivity in $pp \rightarrow hh(j) \rightarrow b\bar{b}\tau^+\tau^-(+j)$ to both di-Higgs production and the trilinear Higgs coupling [19]. This approach is currently also being investigated by ATLAS [20] in the context of an LHC luminosity upgrade.

Crucial to the findings of Ref. [19] is accessing the small invariant di-Higgs mass phase-space region, which

[*]m.j.dolan@durham.ac.uk
[†]christoph.englert@durham.ac.uk
[‡]michael.spannowsky@durham.ac.uk

is mostly sensitive to the Higgs trilinear coupling with moderately boosted Higgses $p_T \sim 100$ GeV. The sensitivity can be augmented by accessing collinear di-Higgs configurations by recoiling the di-Higgs system against a hard jet [19]. This configuration is extremely sensitive to modifications of the trilinear Higgs coupling since it does not suffer from the kinematical shortcomings that are present in the inclusive di-Higgs final state, where the Higgs particles are produced back-to-back. Promising results to measure the di-Higgs cross section have also been found for extremely boosted $b\bar{b}W^+W^-$ production [21].

Motivated by the recently unravelled sensitivity to di-Higgs production at the LHC, we perform a comprehensive and comparative analysis of new-physics interactions in LHC di-Higgs and di-Higgs + jet production in this paper. We divide our discussion into two parts. We discuss resonant di-Higgs(+jet) signatures in Sec. II A, where we first analyze a simple extension of the Higgs sector via the so-called Higgs portal [22]. We subsequently discuss prospects to constrain the minimal supersymmetric SM (MSSM) Higgs sector at low $\tan\beta$ via resonant production of a heavy Higgs H decaying to hh.

In Sec. III we discuss the phenomenology of nonresonant new-physics contributions to di-Higgs production in composite Higgs and dilaton models (to make this work self-contained we briefly introduce the basics before we comment on the phenomenology). This broad class of pseudo-Nambu-Goldstone theories comprises many interesting features in a phenomenologically well-defined framework. Both these models introduce new degrees of freedom to di-Higgs and di-Higgs + jet production and modified trilinear couplings compared to the SM, while the composite Higgs scenarios also introduce new $t\bar{t}hh$ interactions. Comparing these models to the SM expectation provides a consistent framework to constrain the electroweak symmetry-breaking potential with future measurements at the $\sqrt{s} = 14$ TeV LHC.

Throughout this paper, we produce events and leading-order (LO) cross sections using an in-house Monte Carlo code that is based on the VBFNLO [23] and FEYNARTS/FORMCALC/LOOPTOOLS [24] frameworks.

II. RESONANT NEW PHYSICS: FROM THE HIGGS PORTAL TO SUPERSYMMETRY

A. Di-Higgs production in the Higgs portal scenario

The Higgs portal scenario [22] is a convenient and theoretically consistent way to generalize the SM in its mostly unconstrained parameters (such as the Higgs boson's total and hidden decay width) in a minimal approach [25]. Realizing that $\Phi_S^\dagger \Phi_S$ transforms as a gauge singlet, where Φ_S is the SM Higgs doublet, there is a plethora of SM extensions with highly modified and interesting LHC phenomenology [10,11,26]. In a ''mirrored'' approach [27] the Higgs portal potential reads

$$V = \mu_S^2|\Phi_S|^2 + \lambda_S|\Phi_S|^4 + \mu_H^2|\Phi_H|^2 + \lambda_H|\Phi_H|^4$$
$$+ \eta_\theta|\Phi_S|^2|\Phi_H|^2, \tag{2.1}$$

where we have introduced a hidden-sector Higgs field Φ_H. The Higgs portal model allows to identify a viable dark matter candidate in the hidden sector [28], whose potential LHC phenomenology has been explored in Ref. [29].

After symmetry breaking, which is triggered by the Higgs fields acquiring vacuum expectation values (VEVs) $|\Phi_{S,H}| = v_{S,H}/\sqrt{2}$, the would-be-Nambu-Goldstone bosons are eaten by the $W^\pm$, Z fields and the corresponding directions in the hidden gauge sector, and the only effect (in unitary gauge) is a two-dimensional isometry which mixes the visible and the hidden Higgs bosons:

$$h = \cos\theta H_s + \sin\theta H_h,$$
$$H = -\sin\theta H_s + \cos\theta H_h, \tag{2.2}$$

where θ is a function of the portal potential parameters (2.1) (for details see, e.g., Ref. [25]). For the remainder of this section we choose $m_H > m_h = 125$ GeV.

Electroweak precision measurements (for latest results see Ref. [30]) and unitarity requirements of longitudinal gauge-boson scattering and massive-quark annihilation to longitudinal gauge bosons are most efficiently resolved if the mixing is far from maximal, $\cos\theta^2 \approx 1$. This is in agreement with the current rate observations of the Higgs candidate at the LHC. For generic *perturbative* choices of the potential λ_S, λ_V, $\eta_\theta \ll 4\pi$ this results in a typically small mass splitting between the physical Higgs states h, H. Admitting some tuning, a larger mass splitting can be arranged, which results in a clean LHC phenomenology of narrow trans-TeV resonances [31]. Small mass splittings imply a phenomenologically more involved situation since the light Higgs bosons are produced with small transverse momentum in di-Higgs production. Nonetheless, given the vastly enriched Higgs sector phenomenology, we can still study the Higgs portal in sufficient detail to fully reconstruct the Higgs potential (2.1) [25]. Crucial in this reconstruction algorithm is the measurement of the invisible Higgs decay branching ratio [10,32]. It can be immensely improved by a possible observation of a cascade decay $H \to hh$. Additional information from observing all multi-Higgs signatures (and the trilinear couplings especially), if phenomenologically accessible, can be used to further constrain or even rule out the simple portal extension.

Expanding Eq. (2.1) around the vacuum expectation values, we get the trilinear couplings relevant for di-Higgs production[1]:

---

[1]Triple Higgs production—which is sensitive to the modified Higgs quartic couplings—yields phenomenologically irrelevant cross sections, just like in the SM [16].

$$hhh: 3/2(2\lambda_H s_\theta^3 v_H + 2\lambda_S c_\theta^3 v_S + \eta_\theta c_\theta^2 s_\theta v_H + \eta_\theta c_\theta s_\theta^2 v_S), \quad (2.3a)$$

$$HHH: 3/2(2\lambda_H c_\theta^3 v_H - 2\lambda_S s_\theta^3 v_S + \eta_\theta c_\theta s_\theta^2 v_H - \eta_\theta c_\theta^2 s_\theta v_S), \quad (2.3b)$$

$$hHH: 2(3\lambda_H - \eta_\theta)c_\theta^2 s_\theta v_h + 2(3\lambda_S - \eta_\theta)c_\theta s_\theta^2 v_S + \eta_\theta s_\theta^3 v_H + \eta_\theta c_\theta^3 v_S, \quad (2.3c)$$

$$hhH: 2(3\lambda_H - \eta_\theta)c_\theta s_\theta^2 v_H - 2(3\lambda_S - \eta_\theta)c_\theta^2 s_\theta v_S + \eta_\theta c_\theta^3 v_H - \eta_\theta s_\theta^3 v_S, \quad (2.3d)$$

where $c_\theta = \cos\theta$ and $s_\theta = \sin\theta$. Current observations leave open a lot of parameter space for such signatures to be relevant at the LHC. In Fig. 1 we scan over the parameters of the Higgs portal potential enforcing unitarity and electroweak precision constraints, as well as current limits from the ATLAS and CMS experiments [2,3]. If the heavier Higgs mass is $m_H \gtrsim 250$ GeV, there are parameter choices such that the $\sin^2\theta$ suppression of the H decay to SM matter from Eq. (2.2) renders the prompt decay of H to observable SM matter subdominant to the cascade decay $H \to hh$. This can be traced back to large trilinear couplings $\mathcal{O}(v_H, v_S)$ that arise as a consequence of electroweak symmetry breaking. Therefore, there is the possibility to constrain the portal model by measuring the trilinear couplings in resonant and nonresonant $pp \to hh$, hH, $HH + X$ production.

In Fig. 2, we show a scan over the cross sections of $pp \to hh$, hH, $HH \to$ (visible) as functions of the involved trilinear couplings for an exemplary parameter point $v_S \simeq 246$ GeV, $v_H \simeq 24$ GeV, $m_h = 125$ GeV, and $m_H \simeq 255$ GeV, $\Gamma_H = 24$ GeV. This parameter choice implies a large $H \to hh$ branching ratio $\sim 50\%$, which leads to the phenomenological situation that we would like to study in this section. The inclusive cross section for unmodified trilinear coupling values (2.3) at leading order implying (prompt) visible final states are

$$pp \to hh + X: 44.4 \text{ fb}, \quad (2.4a)$$

$$pp \to Hh + X: 5.57 \text{ fb}, \quad (2.4b)$$

$$pp \to HH + X: 667 \text{ ab} \quad (2.4c)$$

(the SM cross section is 16 fb). Comparing to the next-to-leading-order (NLO) QCD corrections in the context of the SM for pure continuum hh production and the MSSM for also assessing the QCD corrections to resonant production by running HIGLU [33] and HPAIR [34], we can expect an enhancement of the cross section by about $K = \sigma^{\text{NLO}}/\sigma^{\text{LO}} \simeq 2$.

For $pp \to hh + j + X$ with $p_{T,j} \gtrsim 80$ GeV we calculate a leading-order cross section of $\sigma = 10.1$ fb (Fig. 3) which should be contrasted to an SM leading-order cross section of $\sigma = 2.58$ fb, which can be isolated from the background [19]. Hence, the measurement of the one jet-inclusive cross section will assist in formulating constraints on such a model.

Note that $pp \to HH + X \to$ visible is naively suppressed $\sim \sin^6\theta$. Therefore, for the bulk of the portal parameter space, heavy di-Higgs production (and di-Higgs + jet production different from $pp \to hh + j + X$) is phenomenologically inaccessible at rates that are too small, with no space left for kinematical signal-over-background (S/B) improvements.

Summary: The Higgs portal scenario offers the possibility of large enhancements in the di-Higgs production rate, from both resonant and nonresonant (via changes in λ_{hhh}) new physics. Extracting the rate for $pp \to h^* \to hh$ using the boosted kinematical techniques from our previous paper [19] along with measuring the resonant peak in the di-Higgs invariant mass spectrum will aid in the full reconstruction of the Higgs portal Lagrangian by correlating these two independent measurements. The general layout of performing such a reconstruction with the help of additional measurements such as invisible decays has been discussed in detail in Ref. [35] for the mirrored model, and we refer the reader to the literature for more information. We note, however, that the reconstruction algorithm does not rely on a measurement of the trilinear coupling. Hence the measurement that we describe can be used to further constrain such a scenario or perform a possible validation in a different search channel. Our strategy is assisted by the cross section's large dependence on λ_{hhh}. A high-luminosity analysis of hh and $hh + j$ production can also facilitate a measurement of the trilinear coupling in this model.
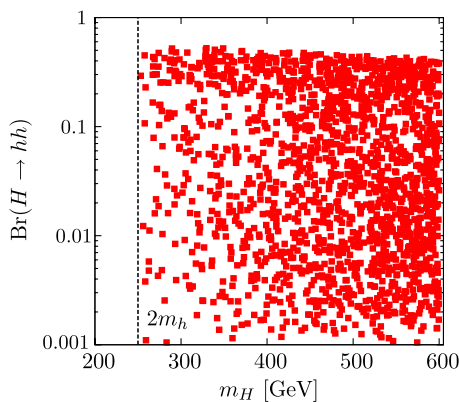

FIG. 1 (color online). Mass of the heavy Higgs state H if $m_h = 125$ GeV, and consistency with S, T, U [81]; unitarity and current ATLAS/CMS results are imposed. The imposed S, T ellipse is taken from Ref. [82]. The density of the model points must not be interpreted as a probability measure and should be interpreted as illustrative because we do not further comment on the dynamics of the hidden sector.
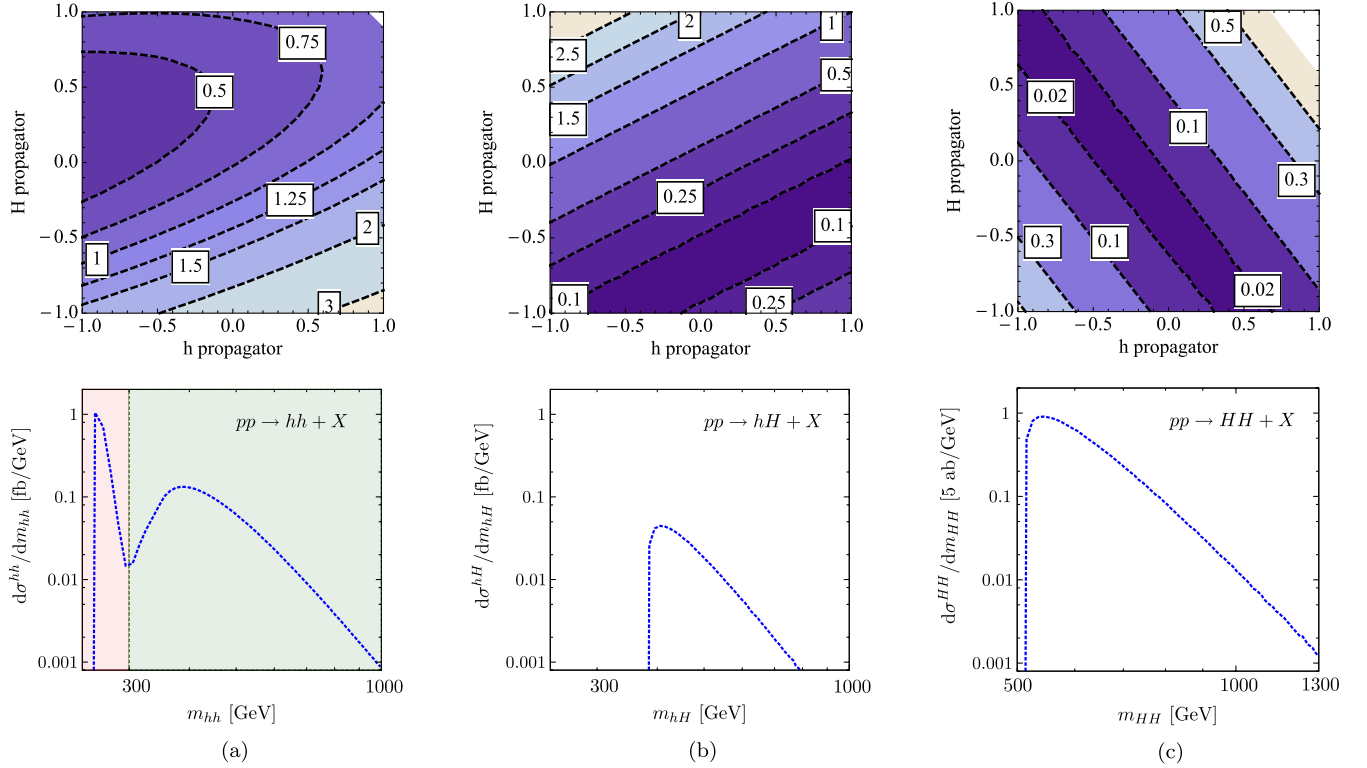
FIG. 2 (color online). Upper panels: cross sections in the portal scenario for the parameter point mentioned in the text. We scan over the multiples of the trilinear couplings Eq. (2.3) that are in one-to-one correspondence with diagrams involving the h, H propagators and show contours relative to the central expectation Eq. (2.4). In panel (a), e.g., "H propagator" amounts to rescaling the Hhh coupling and "h propagator" means rescaling the hhh coupling. Lower panels: invariant di-Higgs mass distributions. (a) σ/σ(portal) and invariant di-Higgs mass distribution for $pp \rightarrow hh + X$ at the LHC 14 TeV. (b) σ/σ(portal) and invariant di-Higgs mass distribution for $pp \rightarrow hH + X$ at the LHC 14 TeV. (c) σ/σ(portal) and invariant di-Higgs mass distribution for $pp \rightarrow HH + X$ at the LHC 14 TeV.

B. The (N)MSSM at small tan β

The Higgs portal model of Sec. II A bears some resemblance to a generic two-Higgs doublet model, and therefore our findings are also relevant for searches for supersymmetry (SUSY) in the context of the MSSM and its extensions.
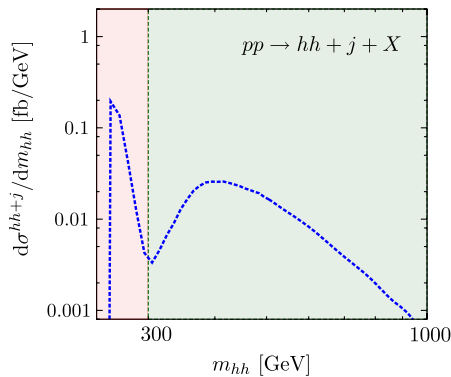

FIG. 3 (color online). Invariant mass distribution for $pp \rightarrow hh + j + X$ in the portal scenario. A cut on the additional jet of $p_T \gtrsim 80$ GeV is imposed.

The trilinear couplings of the Higgs bosons in the MSSM are given by

$$\lambda_{hhh} = 3\cos 2\alpha \sin(\beta + \alpha),$$
$$\lambda_{Hhh} = 2\sin 2\alpha \sin(\beta + \alpha) - \cos 2\alpha \cos(\beta + \alpha), \quad (2.5)$$
$$\lambda_{HHh} = -2\sin 2\alpha \cos(\beta + \alpha) - \cos 2\alpha \sin(\beta + \alpha),$$

up to radiative corrections, details of which can be found in the second reference of Ref. [15], $\tan \beta = v_u/v_d$ is the ratio of VEVs of the two MSSM Higgs doublets, and α diagonalizes the Higgs mixing matrix. The above couplings are in units of $\lambda_0 = M_Z^2/v$. In principle, disentangling the contributions proportional to λ_{Hhh} and λ_{hhh} in double Higgs production would allow a reconstruction of the angles α and β.

We observe that when β is small and we are near the decoupling limit where $\alpha \sim \beta - \pi/2$ then the λ_{Hhh} is proportional to $\cos \beta$. Thus when $2m_h < m_H < 2m_t$ H has a large branching ratio into a pair of Higgses hh, similar to the Higgs portal model in Sec. II A. Probing the di-Higgs final states is thus probably the best way of

finding H if $\tan\beta$ is low. The presence of squarks can further enhance the production by running in the loops.[2]

Achieving a Higgs mass of 125 GeV at such low values of $\tan\beta$ requires exceptionally heavy top-squark masses and mixings. Scanning over the squark masses and mixings, we find that $m_{\tilde{q}} > 50$ TeV in order to achieve $m_h \sim$ 125 GeV. These spectra are characteristic of "mini-split" SUSY, which has recently been advocated in Ref. [37], which suggests that the weak scale is tuned and supersymmetry is present at higher energies. However, it is unusual to have all the scalars heavy except the extra Higgses. This would require the presence of a cancellation between $m_{H_u^2}$ and $m_{H_d}^2$ if these quantities are large like the other scalar soft terms, or else that they have some suppression relative to the squark and slepton masses.

Moving beyond the MSSM, another possibility is that $\tan\beta$ is low and that a large contribution to the mass of the lightest (SM-like) Higgs boson comes from an extra singlet field S with superpotential couplings $\lambda S H_u H_d$. This induces an extra contribution to the Higgs mass $\propto \lambda^2\sin^2 2\beta$ which is enhanced at low $\tan\beta$; this is the so-called λ-SUSY scenario of the next-to-MSSM (NMSSM) [38]. We focus exclusively on the MSSM here; however, we expect the phenomenology to be similar in the NMSSM if the singlet-like states are heavier than the MSSM Higgses.

We find a point with $\tan\beta = 3$, and adjust the scalar masses until we achieve $m_h \sim 125$ GeV. We set the mass of the other CP-even boson of the MSSM H to be 290 GeV. In this regime the branching fraction $\mathrm{BR}(H \to hh) \sim 45\%$, and the decay width is $\Gamma_H = 0.25$ GeV. The other main partial decays are into $b\bar{b}$ (12%), W^+W^- (28%) and ZZ (12%). We could further increase the branching ratio into two Higgses by decreasing $\tan\beta$, at the cost of increasing the scalar masses. Using a suitably modified version of VBFNLO we find the leading-order production cross section $\sigma(pp \to H \to hh) = 246$ fb. We also calculate the cross section for $\sigma(pp \to H \to Hh)$. This is suppressed by the off-shell H in the s-channel, and by the fact that the λ_{HHh} coupling is suppressed relative to the λ_{Hhh} coupling. We find the cross section for this process to be 4.5 fb, too low for observation given that h has SM-Higgs-like branching ratios. We show in Fig. 4 the invariant mass distribution of the di-higgs system for the hh and Hh final states. Similar to the Higgs portal, there is a clear structure of resonant and nonresonant contributions.

We can separate the large contribution $H \to hh$ by reconstructing the di-Higgs invariant mass which exhibits a peak at m_H. This allows us to extract the cross section for $pp \to H \to hh$, and after cutting around the peak the remainder of the events are due to $pp \to h \to hh$. As in the Higgs portal model, this process can be extracted using

---

[2]Note that, depending on the color charge assignment, di-Higgs production can be enhanced compared to single Higgs production [36].
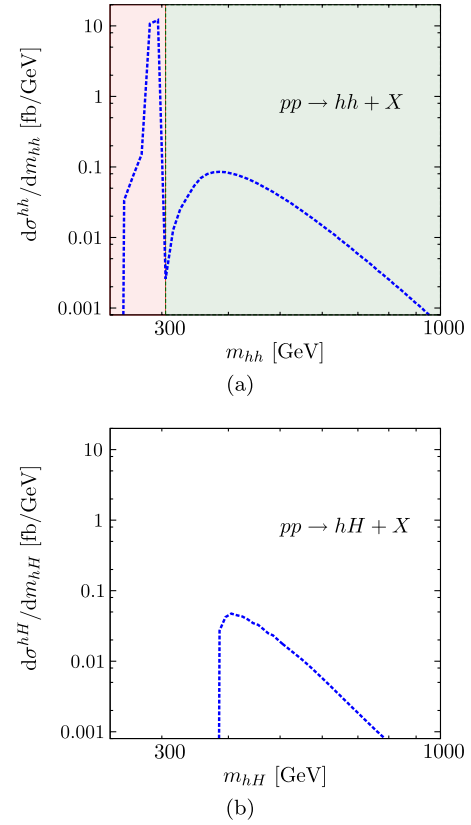

FIG. 4 (color online). Invariant mass distribution of the (a) hh and the (b) Hh system for MSSM-like production at low $\tan\beta$. For details see text.

the techniques from our previous paper, allowing constraints to be put on α and β. The invariant mass distribution and rate for the $hh + j$ final state are also similar to the portal scenario (Fig. 3).

Summary: The di-Higgs phenomenology in the MSSM at low $\tan\beta$ is similar in many respects to that of the Higgs portal model. Measurements of the resonant and nonresonant contributions to di-Higgs production allows a reconstruction of the parameters α and β.

III. NONRESONANT NEW PHYSICS: PSEUDO-NAMBU-GOLDSTONEISM

Apart from softly broken supersymmetry, strong interactions are the only other constructions which can cure the naturalness problem (if only partially).

A well-known example of electroweak symmetry breaking from strong interactions is technicolor (TC) where $m_W \sim f$, where f is the "pion" decay constant. The techni-Σ and techni-ρ resonances will have masses of the order of the TC confining scale, which should be low in order to maintain perturbative longitudinal gauge-boson scattering. However, if this is the case then these states generally give large contributions to the precision

electroweak S-parameter. An illustrative example which incorporates such a light (vector) resonance is easily constructed from the holographic interpretation of a bulk gauge theory broken by boundary conditions in a Randall-Sundrum background [39][3]: The appearance of the infrared brane signals the spontaneous breakdown of conformal invariance in the dual picture [41]. This is accompanied by the Higgsing of a bulk gauge symmetry, which corresponds to breaking a weakly gauged global symmetry in the strongly interacting conformal field theory (CFT). Upon stabilizing the compactification moduli via the Goldberger-Wise mechanism [42] the zero-mass radion is lifted, which couples to the conformal anomaly:

$$T_\mu^\mu \sim m_W^2 W_\mu^+ W^{-\mu} + \frac{m_w^2}{\cos^2\theta_w} Z_\mu Z^\mu + \sum_f m_f \bar{f} f + \cdots.$$

$$(3.1)$$

In the CFT picture we identify a pseudodilaton, which has an impressive resemblance to the SM Higgs boson as a consequence of its couplings. In this sense, the dilaton mimics a light Higgs boson because the mass terms are the source of the scaling violation.

Different to this approach is the idea of the entire Higgs multiplet as a set of Nambu-Goldstone bosons. There are multiple ways to construct such a model consistently, ranging from early ideas such as Ref. [43], to collective symmetry breaking [44], holographic Higgs models [45,46] and other modern approaches [47] which vary in their details and symmetry content. Common to all these realizations is the breaking of a global symmetry pattern by gauging a subgroup of the strongly interacting sector.

While there are parameter choices for both scenarios which are consistent with the SM in their *single* Higgs phenomenology, the measurement of the di-Higgs(+jet) production can be a key discriminator between these different nonresonant realizations.

A. Di-dilaton production

We first discuss the implications of interpreting the 125 GeV boson as a pseudodilaton [48,49]. We note that there is a substantial number of options in modelling the electroweak sector using strong interactions, and thus the conclusions of this section should be taken as illustrative rather than definitive for this class of models.

The pseudodilaton is associated with the spontaneous breaking of scale symmetry at an unknown scale f, and we denote this field by χ. The couplings of the pseudodilaton to massive Standard Model particles are determined by its coupling to the trace of the SM energy-momentum tensor $T_{\mu\nu}$, Eq. (3.1). The couplings of the pseudodilaton to the

massive SM particles are thus the same as those of the SM Higgs, but rescaled by a factor of v/f [48–50]. The couplings of the pseudodilaton to gluons and photons are given by

$$\mathcal{L}_{\chi,\text{massless}}^{D5} = \frac{\alpha_{\text{EM}}}{8\pi f} c_{\text{EM}} \chi F_{\mu\nu} F^{\mu\nu} + \frac{\alpha_{\text{S}}}{8\pi f} c_{\text{S}} \chi G_{\mu\nu}^a G^{a\mu\nu},$$

$$(3.2)$$

where $c_{\text{EM,S}}$ are anomaly coefficients. The precise values these take depends on what further assumptions are made about the UV dynamics of the theory and what heavy colored and electromagnetically charged states are present. We assume that the dilaton couples to photons and gluons via the full QCD/EM beta function [50,51]. We also consider the model of Ref. [52] which studies the same system with an extra family of quarks. In both these cases we can find SM-like behavior with an enhanced $\sigma \times \text{BR}$ into photon pairs.

In the fully composite scenario, the dilaton couples to massless gauge bosons via the full beta function, and we have $c_{\text{EM}} = -17/9$ and $c_{\text{S}} = 11 - 2n_f/3$, where $n_f = 5$ [50] is the number of light quarks. In the four-family model we have $c_{\text{EM}} = -6/5$ and $c_{\text{S}} = 4/3$, and obtain a similar single-dilaton phenomenology. The production cross section of the dilaton can be enhanced by orders of magnitude relative to the SM value. However, as the dominant decay channel then becomes $\chi \to gg$, the cross section times branching ratio of the observable final states $\chi \to f\bar{f}$, $\chi \to VV$ and $\chi \to \gamma\gamma$ can still be close to their SM values, depending on the scale f (following arguments similar to the ones presented in Refs. [10,53,54]).

There will also generally be dimension-six operators, the most interesting of which is [55]

$$\mathcal{L}^{D6} = -\frac{\alpha_{\text{S}}}{4\pi f^2} c_{\chi\chi GG} \chi^2 (G_{\mu\nu}^a)^2. \qquad (3.3)$$

We define the $D6$ operator with a minus sign, so that $c_{\chi\chi GG} > 0$ complies with the low-energy effective-Higgs-theorems [33,56,57] paradigm: integrating out the heavy top quark, we obtain an effective interaction $\mathcal{L} \sim G_{\mu\nu}^a G^{a\mu\nu} \log(1 + h/v)$ in the SM.

It is important to keep in mind that the higher-dimensional interactions with the gluon and the photon fields arise from integrating out the conformal dynamics and need not follow the linear energy transfer (LET) paradigm, which predicts a unique coupling structure of the $h^n G_{\mu\nu}^{a2}$ interactions as a consequence of $m \propto \langle h \rangle$ for all fundamental masses in the SM.[4] We also explore the possibility that the dimension-six operator is negligible by setting $c_{\chi\chi GG} = 0$.

---

[3]Owing to the large-N and large-'t Hooft coupling limit [40] of AdS/CFT, it is intrinsically difficult to construct a fully realistic model in terms of electroweak precision measurements.

[4]There is in fact a connection between LET and the vanishing trace anomaly (3.1) for infrared photons, $\lim_{Q^2 \to 0} \langle 0|T_\mu^\mu|\gamma\gamma \rangle = 0$ [56,58].
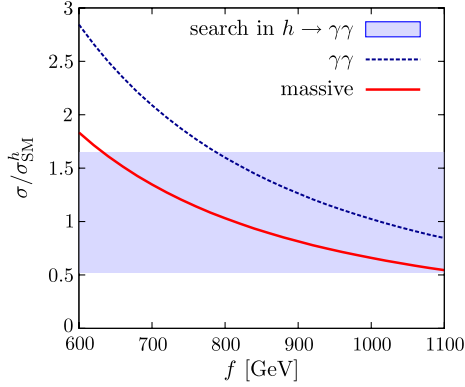
FIG. 5 (color online). Dilaton production from gluon fusion with current limits of the $h\gamma\gamma$ coupling analysis [6] included.

For the fully composite model we find that for $f = 850$ GeV the $\sigma \times$ BR of the dilaton into massive final states is very similar to those in the Standard Model, and $\chi \to \gamma\gamma$ is 1.55 times the Standard Model value. For gluons we find that $\sigma \times$ BR is enhanced by a factor of approximately 150. This agrees with values obtained from recent fits of experimental data in Refs. [5,6,48]. We show in Fig. 5 the $\sigma \times$ BR for massive states and for $\gamma\gamma$, normalized to the SM values. We also include a blue horizontal band indicating the signal strength in the diphoton channels from combining the ATLAS and CMS searches [2,3]. In the four-family case we obtain similar results for $f \sim 570$ GeV.

The dilaton's total decay width is approximately 5 MeV, which is very similar to the SM. Upper limits on the Higgs width are difficult to assess experimentally [59] and will eventually be limited by large systematic uncertainties [60]. Constraints on the dilaton model arising from such measurements will be too loose to rule this model out. As we will see, investigating multidilaton production provides the missing handle to constrain the model when consistency with single-Higgs observations prevails.

We introduce explicit sources of scale symmetry breaking [50] through the operator $\lambda_{\mathcal{O}}\mathcal{O}(x)$, where the scaling dimension of the operator $\mathcal{O} \neq 4$ induces nonderivative trilinear interactions for χ. When the operator $\mathcal{O}$ is nearly marginal, one writes the trilinear coupling as $\frac{\lambda}{6}\frac{m_\chi^2}{f}\chi^3$ and obtains for λ

$$\lambda = (\Delta_{\mathcal{O}} + 1) + \cdots, \qquad \lambda_{\mathcal{O}} \ll 1, \qquad (3.4)$$

where we must have $\lambda \geq 2$ by the conformal algebra and unitarity. If $\Delta_{\mathcal{O}} = 2$ we obtain the Standard Model result, rescaled by the ubiquitous factor of v/f. Another possibility is when $\gamma \ll 1$, where one obtains $\lambda = 5$, which is 66% larger than the SM trilinear up to factors of v/f. There are also interesting anomalous four-derivative interactions in the low-energy dilaton theory [61,62],

TABLE I. Parameters used in the calculation of double dilaton production in Sec. III A

Parameter	Value	Parameter	Value
f	850 GeV	λ	3 (SM)
c_S	7 (4/3)	c_{EM}	$-17/9$ (-1.2)
Δa	0.05 (0.2)	$c_{\chi\chi GG}$	(0)

$$\mathcal{L}^{D7,D8} \supset 2(a_{UV} - a_{IR})(2(\partial\chi)^2 \Box \chi - (\partial\chi)^4), \quad (3.5)$$

of which the first gives rise to a trilinear interaction. As these interactions are derivative their largest effects will be seen in the high-p_T regime, which we exploited in Ref. [19] in order to suppress backgrounds to a manageable level. If we consider a strongly interacting SU(N) gauge theory, then there will be $N^2 - 1$ gauge fields, and the theory will be approximately conformal if there are $\sim 11N$ flavors of Weyl fermion. Taking $N = 4$, 5,6 we obtain $a_{UV} = 0.033$, 0.053 and 0.076, using the results in Ref. [61]. We will initially take $\Delta a = a_{UV} - a_{IR} = 0.05$, but we also consider a "large"-anomaly-coefficient scenario, where we take $\Delta a = 0.2$.

We summarize the parameter values we use regarding double dilaton production in Table I, and show $c_{\chi\chi GG}$ in brackets to indicate that we usually use the value derived by matching with the effective field theory, but sometimes switch its effect off altogether.

Figure 6 shows the differential distribution of $\sigma \times$ BR for a number of final states, normalized to those of the SM, in both the low- and high-anomaly-coefficient scenarios. The lower panels show the fully composite SM and the upper ones the four-family scenario. The effects of the higher-dimensional operators changing the p_T spectrum can be seen entering at around 150 GeV. In the fully composite case, while the cross section for those final states involving either two or four gluons are boosted with respect to the SM, the final states that have proved useful in previous di-Higgs analyses are suppressed relative to the SM, even though the total cross section for $\chi\chi$ is considerably higher. This is due to the double suppression coming from the factor v^2/f^2 associated with massive final states. Although the $\gamma\gamma jj$ final-state cross section is ten times the SM rate, the leading-order background is still too large to make an effective analysis. As it will never be feasible to pick out the relatively few $gggg$ or $bbgg$ events from the enormous QCD background, one does not expect any signal for this particular scenario. One possible exception is in the very boosted regime where $p_{T,\chi} \geq 350$ GeV, if the effects of higher-dimensional operators are large.

On the other hand, the suppression factor into massive states is smaller in the four-family case than in the fully composite case, and the overall branching ratios are more similar to their SM values. While the extra colored states
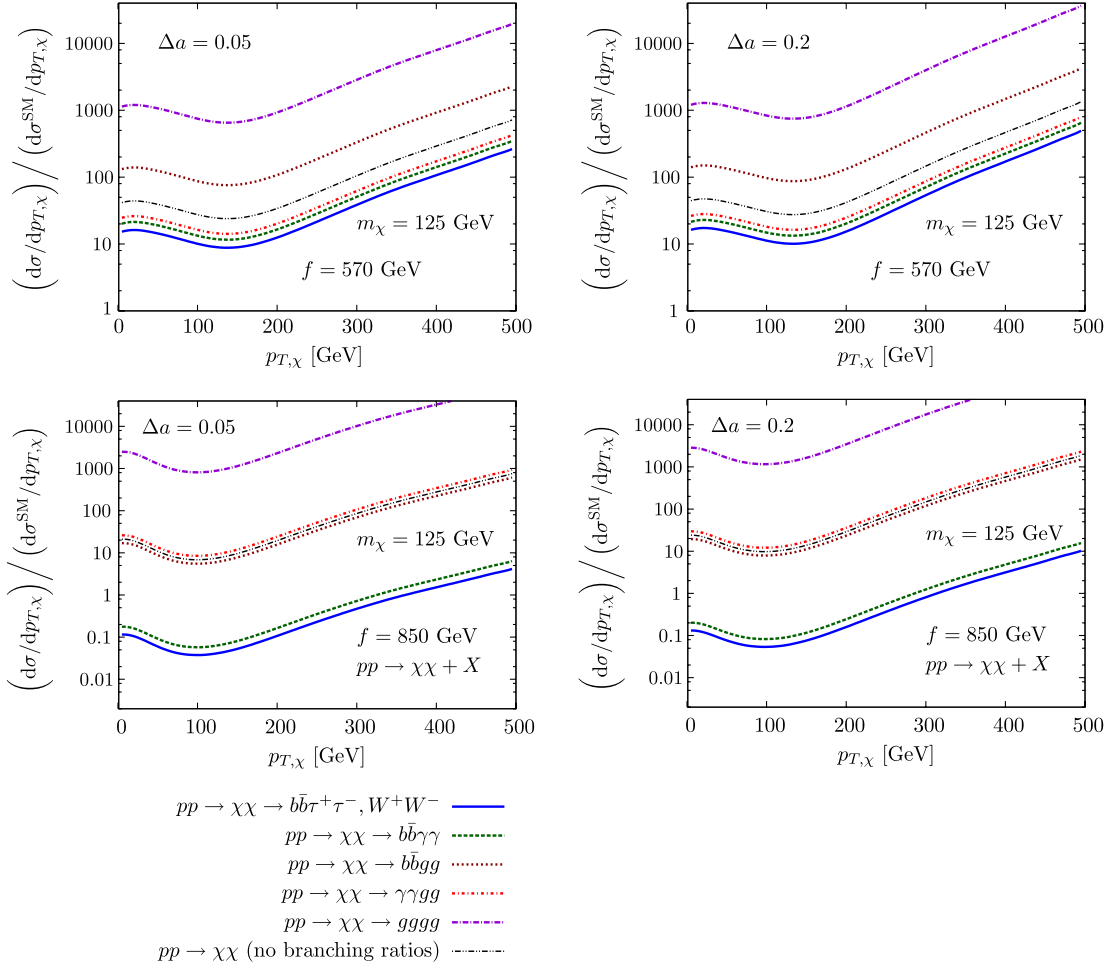
FIG. 6 (color online). Comparison of $\sigma(\chi\chi) \times \mathrm{BR}(\chi_1)\mathrm{BR}(\chi_2)$ to the values of the SM as a function of $p_{T,\chi}$ for $\Delta a = 0.05$ (left panel) and $\Delta a = 0.2$ (right panel) and $c_S = 7$, $c_{\chi\chi GG} = 1$. The upper panels are for $f = 570$ GeV, and the lower ones for $f = 850$ GeV. The comparison of $\Delta a = 0.05, 0.2$ is depicted in Fig. 7.

enhance the total rate, the branching ratio to gluons is not so enhanced so as to render an analysis impossible. On the contrary, $\sigma \times \mathrm{BR}$ for $bb\tau\tau$ and bbW^+W^- is approximately an order of magnitude larger than in the SM, a factor which is enhanced even more in the high-p_T tail of the distribution.

In Fig. 7 we show the effects on the p_T differential distribution of varying the anomaly coefficient Δa and the dimension-six coefficient $c_{\chi\chi GG}$, relative to the "standard" case with $\Delta a = 0.05$. The yellow line includes only the anomalous derivative couplings which appeared in the proof of the a-theorem. Its effect is similarly boosted in the low-p_T region where there is a lack of destructive interference due to the absence of extra box diagrams. We see that the effects of these interactions becomes important for $p_{T,\chi} \sim 350$ GeV, where it can change the cross section by a factor of a few. The prospects for using the di-dilaton final state to constrain the properties of the theory's UV completion are thus promising.
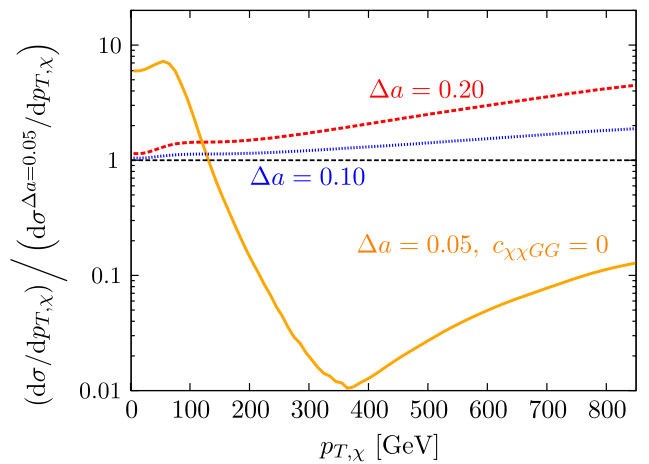

FIG. 7 (color online). Comparison of $\sigma(\chi\chi)$ for different values of Δa and $c_{\chi\chi GG}$ as a function of $p_{T,\chi}$ for $c_S = 7$, $f = 850$ GeV fixed. The blue dotted line marked $\Delta_a = 0.10$ gives a comparison of $\Delta a = 0.1$ to $\Delta a = 0.05$ for fixed c_S and $c_{\chi\chi GG}$.

Summary: The cross section for di-dilaton production is much larger than in the Standard Model. However, the future LHC prospects for this scenario exhibit a strong dependence on one's assumptions about the UV properties of the theory. In the fully composite SM, when the suppression associated with nongluonic final states is taken into account, all possibly observable final states are too suppressed by their branching ratios to give a signal at the LHC. On the other hand, in the four-family scenario the prospects are excellent, with the cross section for reconstructible final states enhanced by up to an order of magnitude. This is large enough that one may begin to constrain further facets of the UV theory which manifest themselves through higher-dimensional operators.

B. Composite di-Higgs production

The other possible way to have a light SM-like Higgs boson that we discuss in this work is the composite Higgs scenario. The composite Higgs [43,46,47,63] is the realization of the Higgs as a Nambu-Goldstone boson of a broken global symmetry of some strongly interacting gauge theory. The electroweak interactions are then gauged as a subgroup of this larger spontaneously broken global symmetry group, e.g.,

$$\mathrm{SO}(5) \to \mathrm{SO}(4) \simeq \mathrm{SU}(2)_L \times \mathrm{SU}(2)_R, \qquad (3.6)$$

which contains the gauged $\mathrm{SU}(2)_L$. Gauging a subgroup is tantamount to explicit breaking of the global symmetry after which some of the Nambu-Goldstone bosons gain masses. The (uneaten) Nambu-Goldstone bosons that arise from global symmetry breaking pick up masses from the Coleman-Weinberg potential [64] and break electroweak symmetry [63,65,66]. This mechanism is elegantly described by holographic approaches [45], where symmetry breaking is realized via the Hosotani mechanism [67] in gauge-Higgs unified models.

To incorporate proper hypercharges we need to extend the symmetry group to $\mathrm{SO}(5) \times \mathrm{U}(1)_X$, and we identify hypercharge as $Y = X + T_R^3$ like in other models of strong symmetry breaking [39].

The crucial parameter that measures deviations of the physical Higgs' couplings to SM matter and parametrizes the model's oblique corrections is given by $\xi = v^2/f^2$, where f is the analogue to the pion decay constant. Consistency with experimental data can be achieved without much tuning (for a recent analysis see Ref. [68]), which makes this model class a promising candidate for a BSM Higgs sector. In these modern composite Higgs models one generates fermion masses via linear mixings with composite fermionic operators instead of Technicolor-type interactions to avoid bounds $\xi \ll 1$. In total, this amounts to a highly modified di-Higgs phenomenology compared to the SM expectation, which has already been discussed in Refs. [69–72] in some detail. In Ref. [73], the effects of the light additional fermionic degrees of freedom in the

minimal composite Higgs model based on Eq. (3.6) (referred to as MCHM5) have been included to inclusive di-Higgs predictions beyond LET (see also Ref. [74]). The additional fermions that run in the gluon fusion loops strongly enhance the cross section, and, therefore, can be highly constrained by applying the strategies that involve jet recoils in di-Higgs production discussed in our previous paper [19] as we will see below.

MCHM5 introduces a set of composite vector-like fermions that form a complete 5 under SO(5). The 5 decomposes under the unbroken $\mathrm{SU}(2)_L \times \mathrm{SU}(2)_R$, $\psi \equiv 5_{2/3} = (2, 2)_{2/3} + (1, 1)_{2/3}$. Obviously, the $5_{2/3}$ contains a weak doublet of fields with the same quantum numbers as the left-handed SM quark doublet $q_L = (t_L, b_L)^T$ and right-handed top quark, and we can interpret the large mass of the top quark as a mixing effect,

$$\begin{aligned} -\mathcal{L}_m = {} & yf(\bar{\psi}_L \Sigma^T)(\Sigma \psi_R) + m_0 \bar{\psi}_L \psi_R \\ & + \Delta_L \bar{q}_L Q_R + \Delta_R \bar{\tilde{T}}_L t_R + \mathrm{H.c.}, \qquad (3.7\mathrm{a}) \end{aligned}$$

where the nonlinear Higgs field Σ is parametrized via the SO(5)/SO(4) coset-space generators and can be chosen by (see, e.g., Ref. [73])

$$\Sigma = (0, 0, \sin(h/f), 0, \cos(h/f)). \qquad (3.7\mathrm{b})$$

Expanding the nonlinear sigma model we recover the interactions with electroweak gauge bosons as well as the Higgs self-couplings relevant to this study,

$$\begin{aligned} \mathcal{L}_h = {} & \frac{1}{2}(\partial_\mu h)^2 - \frac{m_h^2}{2} h^2 - \frac{1 - 2\xi}{\sqrt{1 - \xi}} h^3 + \cdots \\ & + \frac{g^2 f^2}{4} \sin^2\!\left(\frac{h}{f}\right)\!\left(W_\mu^+ W^{-\mu} + \frac{1}{\cos^2\theta_w} Z_\mu Z^\mu\right), \quad (3.8) \end{aligned}$$

where we have $f^2 \sin^2(\langle h\rangle/f) = v^2$, and thus we need to rescale the SM trilinear hVV vertices by a factor of $\sqrt{1 - \xi}$.

Following Ref. [73], we do not include another $5_{-1/3}$ multiplet for generating the bottom-quark mass, but include it by breaking partial compositeness with an explicit coupling of the Yukawa-like interactions. Expanding Eq. (3.7) in the mass-diagonal basis, we obtain the masses of the fermionic mass spectrum and interactions $h\bar{f}_i f_j$ and $hh\bar{f}_i f_j$ (where i, j run over the heavy fermion flavors) which are relevant for di-Higgs(+jet) production from gluon fusion, which is the dominant production mechanism.[5] The Higgs branching ratios of MCHM5 are depicted in Fig. 9.

---

[5] Di-Higgs production from weak boson fusion [75] is suppressed as well because in addition to the hVV vertices the $hhVV$ vertices are rescaled by $1 - 2\xi$ with respect to the SM. The unitarization of the $V_L V_L \to V_L V_L$, $q\bar{q}$ amplitudes is partially taken over by the exchange of techni-ρ like resonances. These can be studied in the weak boson fusion channels [76–78].
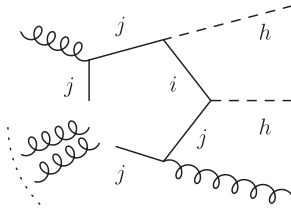
FIG. 8. Schematic representation of the $2h + ng$ irreducible one-loop (sub)amplitude and for the involved fermion flavors in MCHM5. The gluon lines should be understood as off-shell currents contributing to, e.g., $q\bar{q} \rightarrow hhg$. The amplitudes involving the trilinear Higgs vertex [i.e., the irreducible $h + ng$ (sub) amplitudes] are flavor diagonal due to diagonality at the gluon vertices $\not{A}\bar{f}_i f_j \propto \delta_{ij}$. We include all partonic subprocesses in our calculation.

In general, the composite Higgs interactions (3.7) will not be flavor-diagonal in the space of states that contains the composite multiplet augmented by $t_{L,R}$, and constraints from both direct detection and flavor measurements are eminent. For the remainder of this section we will choose parameter points that are in agreement with these constraints to discuss the composite Higgs model's implications on di-Higgs and di-Higgs + jet phenomenology, following Ref. [73].

We take into account all nondiagonal couplings and keep the full mass dependence in the calculation beyond any approximation. This results in computationally intense calculations, especially for the pentagon part in $gg \rightarrow ghh$ and box $gg \rightarrow hh$ (sub)amplitudes where nondiagonality of the $h\bar{f}_i f_j$ vertices increases the Feynman-graph combinatorics (Fig. 8).

The result in comparison to the SM is shown in Fig. 10 for $pp \rightarrow hh + X$ production. For a mass spectrum $m_t \simeq 174$ GeV and the lightest composite fermion
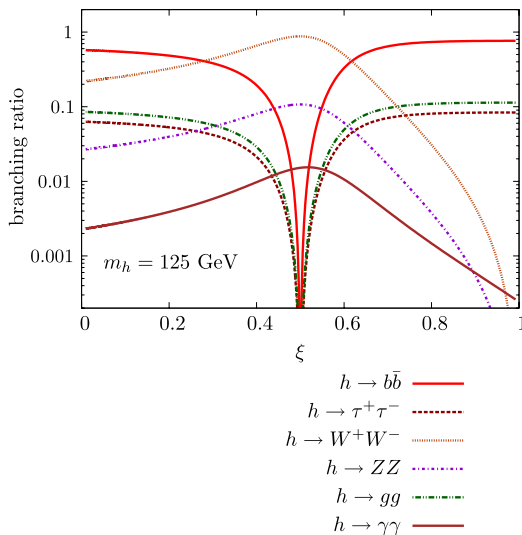
$m_{\text{lightest}} \simeq 1500$ GeV we find agreement with the enhanced cross sections as reported in Ref. [73], $\sigma(hh)/\sigma^{\text{SM}}(hh) \sim 3$, which are shown by the horizontal lines. We also include the case when $m_{\text{lightest}} = 2.0$ TeV. The phase-space dependence of this enhancement is rich and nontrivial as a consequence of the nondiagonal couplings and additional mass scales that show up in the box contributions, which also interfere with modified trilinear interactions. Hence, it is difficult to comment on quantitative similarities of the composite Higgs phenomenology for different parameter choices.

However, on a qualitative level, since the composite scale typically needs to be large in order to have agreement with direct searches and flavor bounds, the inclusive $pp \rightarrow hh + X$ composite phenomenology will be dominated by modifications with respect to the SM at medium $p_{T,h} \simeq 100$ GeV. This phase-space region is mostly sensitive to modifications of the tth coupling and the modified trilinear h vertex. At large $p_{T,h}$ we observe an enhancement due to the presence of new massive fermions in the box contributions of the $\overset{(-)}{q}g$-initiated subprocesses, which access the protons' valence-quark distribution. We note that higher-order QCD corrections are likely to further enhance the cross section prediction beyond the naive SM rescaling [34,79].

We find an even larger enhancement of the leading-order $pp \rightarrow hh + \text{jet}$ production cross section, with $p_{T,j} \gtrsim 80$ GeV,
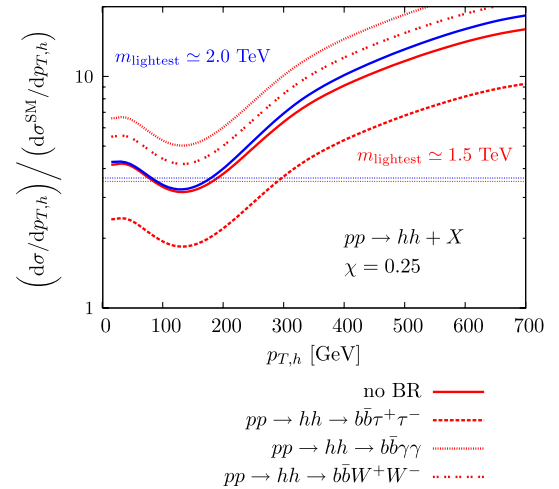
$$\sigma(hh + j) \simeq 13.0 \text{ fb}, \tag{3.9}$$

FIG. 10 (color online). Comparison of composite di-Higgs production $p_{T,h}$ spectra with the SM for $\xi = 0.25$. The red colored lines are for the $m_{\text{lightest}} = 1.5$ TeV case, where the solid line is without branching ratios, and the dotted and dashed lines include the effects of branching ratios. We also include a blue (upper solid) line for m_{lightest} to demonstrate the enhanced cross section at high p_T as described in the text. The two horizontal lines show the ratio of the total cross section to the SM cross section.

FIG. 9 (color online). Branching ratios for the $m_h = 125$ GeV Higgs as a function of χ in MCHM5.

for both scenarios shown in Fig. 10. This result needs to be compared to the corresponding LO prediction in the SM, which is $\sigma^{SM} = 2.8$ fb, and amounts to an enhancement of a factor of 4.6. For the fully hadronized $bb\tau\tau + j$ search of Ref. [19] this amounts to $S/B \simeq 7$, which is well beyond systematic background uncertainties for high-luminosity searches.

The relatively larger increase of the one jet-inclusive cross section can be understood along the following lines. The additional top partners introduce a new mass scale to the one-loop amplitude. At large transverse momentum, the cross section is dominated by continuum hh production which mostly proceeds via box diagrams in addition to initial radiation. The latter is increased as a result of the newly introduced mass scale in comparison to the SM, and initial-state radiation allows the initial-state partons to access the large valence-quark parton distributions. This effect is also visible in the NLO predictions of $pp \rightarrow hh + X$ in composite models employing the effective theory approximation [79].

Summary: The composite Higgs scenario is a well-motivated model of electroweak symmetry breaking that is consistent with current flavor constraints and direct searches for heavy top partners. Furthermore, composite Higgs models typically predict a large enhanced di-Higgs cross section, which is further enhanced for the $hh +$ jet final state by the introducion of a new mass scale to the phenomenology. While small di-Higgs(+jet) rates in the context of the SM might hinder a determination of the SM Higgs potential in case no further indications of physics beyond the SM become available, composite di-Higgs production will overcome this shortcoming due to its large production cross section. Consequently, also for extremely heavy top partners, di-Higgs(+jet) production is going to provide a powerful test of Higgs compositeness at the LHC.

IV. CONCLUSIONS

A precise determination of the realization of the Higgs mechanism *sui generis* is an important task that has to be pursued at the LHC, especially after the recent discovery of an SM Higgs-like particle. While measurements based on single Higgs boson production provide only indirect constraints on the realization of electroweak symmetry breaking, the partial experimental reconstruction of the Higgs potential is indispensable to gain a fuller understanding at a more fundamental level.

In this paper, we have investigated di-Higgs and di-Higgs + jet production in a variety of model classes, whose single Higgs production characteristics can account for the observation of the new particle at the LHC. Rather than employing an agnostic field theory approach,[6] we have picked well-motivated examples of realistic BSM (scalar) sectors, supplemented by the required fermionic

particle content, which generalize the SM Higgs sector in two fundamentally distinct ways.

The first option deals with models with extended Higgs sectors predicting new resonant structures in di-Higgs production due to the model's two-Higgs doublet character, which can provide extra analytical handles via the production of a heavy Higgs boson in addition to the usual light Higgs. In portal-inspired scenarios, the determination of the involved trilinear couplings is important for the reconstruction of the full extended portal potential. In the MSSM, a corresponding measurement facilitates the reconstruction of the Higgs-sector mixing angles α and β, and hence provides indirect constraints on the top-squark masses and mixing parameter A_t. This could be achieved by separating the resonant contribution from continuum production via invariant mass cuts, and applying boosted [19] and unboosted [17] analysis strategies to the different samples.

The resonant models are contrasted to realizations of the Higgs mechanism where the ''Higgs'' boson arises as a pseudo-Nambu-Goldstone mode of some spontaneously broken symmetry. The agreement of current observations with the SM Higgs predictions requires the pseudo-Nambu-Goldstone boson to have similar couplings as the SM Higgs boson. Along with composite Higgs models this leaves only the pseudodilaton as a second option.

The former (composite) case implies interpreting the entire Higgs doublet as a set of Nambu-Goldstone fields. Realistic composite Higgs scenarios predict strongly enhanced di-Higgs and di-Higgs + jet cross sections.

In models with an approximate conformal invariance, symmetry breaking can be triggered at scales considerably higher and spontaneous breaking of conformal invariance introduces a new light state to the low-energy effective theory, which has similar properties as the SM Higgs boson as a consequence of Eq. (3.1): the pseudodilaton. Pseudo-di-dilaton production can be buried in a large hadronic background with no kinematic handles to reconstruct the preferred dilaton decay to gluons. In this sense, the absence of a ''traditional'' di-Higgs phenomenology could be interpreted as evidence for a dilatonic realization. Interpreting the presence of a large di − Higgs(+jet) production cross section is more involved, and could be evidence for a fourth-family (or more complicated) realization of the pseudodilaton model, but may also be consistent with a composite Higgs.

For both the composite and the dilaton option, there are parameter choices such that current observations can be accounted for. It is their highly modified di-Higgs phenomenology which can effectively discriminate between these possibilities depending on the further particularities of the conformal sector, and facilitates an LHC measurement of the involved couplings and parameters in the case of the composite Higgs model.

It is clear from our analysis that, no matter what governs the dynamics of the newly discovered boson, its

---

[6]See Ref. [80] for related discussions.

multiproduction phenomenology—which can be studied at the LHC in sufficient detail—will provide a clear image of its role in the mechanism of electroweak symmetry breaking. These findings will further consolidate with an LHC luminosity upgrade [20].

[1] F. Englert and R. Brout, Phys. Rev. Lett. **13,** 321 (1964); P. W. Higgs, Phys. Lett. **12,** 132 (1964); Phys. Rev. Lett. **13,** 508 (1964); G. S. Guralnik, C. R. Hagen, and T. W. B. Kibble, Phys. Rev. Lett. **13,** 585 (1964).

[2] G. Aad *et al.* (ATLAS Collaboration), Phys. Lett. B **716,** 1 (2012).

[3] S. Chatrchyan *et al.* (CMS Collaboration), Phys. Lett. B **716,** 30 (2012).

[4] Tevatron New Phenomena and Higgs Working Group (TEVNPH), for the CDF and D0 Collaborations, arXiv:1203.3774.

[5] A. Azatov, R. Contino, and J. Galloway, J. High Energy Phys. 04 (2012) 127; D. Carmi, A. Falkowski, E. Kuflik, T. Volansky, J. Zupan, P. P. Giardino, K. Kannike, M. Raidal, and A. Strumia, Phys. Lett. B **718,** 469 (2012); J. Ellis and T. You, J. High Energy Phys. 09 (2012) 123; J. R. Espinosa, C. Grojean, M. Muhlleitner, and M. Trott, J. High Energy Phys. 12 (2012) 045.

[6] T. Plehn and M. Rauch, Europhys. Lett. **100,** 11002 (2012).

[7] O. Buchmueller *et al.*, Eur. Phys. J. C **72,** 2020 (2012).

[8] R. Barate *et al.*, Phys. Lett. B **565,** 61 (2003).

[9] The ATLAS collaboration, Report No. ATLAS-CONF-2012-127.

[10] C. Englert, J. Jaeckel, E. Re, and M. Spannowsky, Phys. Rev. D **85,** 035008 (2012).

[11] C. Englert, M. Spannowsky, and C. Wymant, Phys. Lett. B **718,** 538 (2012).

[12] B. A. Dobrescu, G. L. Landsberg, and K. T. Matchev, Phys. Rev. D **63,** 075003 (2001); A. Falkowski, D. Krohn, L.-T. Wang, J. Shelton, and A. Thalapillil, Phys. Rev. D **84,** 074022 (2011); C.-R. Chen, M. M. Nojiri, and W. Sreethawong, J. High Energy Phys. 11 (2010) 012.

[13] I. Lewis and J. Schmitthenner, J. High Energy Phys. 06 (2012) 072; M. Baumgart and A. Katz, J. High Energy Phys. 08 (2012) 133.

[14] C. Englert, T. S. Roy, and M. Spannowsky, Phys. Rev. D **84,** 075026 (2011).

[15] E. W. N. Glover and J. J. van der Bij, Nucl. Phys. **B309,** 282 (1988); T. Plehn, M. Spira, and P. M. Zerwas, Nucl. Phys. **B479,** 46 (1996); **B531,** 655(E) (1998); S. Dawson, S. Dittmaier, and M. Spira, Phys. Rev. D **58,** 115012 (1998); A. Djouadi, W. Kilian, M. Muhlleitner, and P. M. Zerwas, Eur. Phys. J. C **10,** 45 (1999).

[16] T. Plehn and M. Rauch, Phys. Rev. D **72,** 053008 (2005).

[17] U. Baur, T. Plehn, and D. L. Rainwater, Phys. Rev. D **69,** 053004 (2004).

[18] J. M. Butterworth, A. R. Davison, M. Rubin, and G. P. Salam, Phys. Rev. Lett. **100,** 242001 (2008); T. Plehn, G. P. Salam, and M. Spannowsky, Phys. Rev. Lett. **104,** 111801 (2010); A. Abdesselam *et al.*, Eur. Phys. J. C **71,** 1661 (2011); A. Altheimer *et al.*, J. Phys. G **39,** 063001 (2012).

[19] M. J. Dolan, C. Englert, and M. Spannowsky, J. High Energy Phys. 10 (2012) 112.

[20] The ATLAS collaboration, Report No. ATL-PHYS-PUB-2012-004.

[21] A. Papaefstathiou, L. L. Yang, and J. Zurita, Phys. Rev. D **87,** 011301 (2013).

[22] For early work see T. Binoth and J. J. van der Bij, Z. Phys. C **75,** 17 (1997); B. Patt and F. Wilczek, arXiv:hep-ph/0605188; R. Schabinger and J. D. Wells, Phys. Rev. D **72,** 093007 (2005).

[23] K. Arnold *et al.*, Comput. Phys. Commun. **180,** 1661 (2009).

[24] T. Hahn, Comput. Phys. Commun. **140,** 418 (2001); T. Hahn and M. Perez-Victoria, Comput. Phys. Commun. **118,** 153 (1999).

[25] C. Englert, T. Plehn, M. Rauch, D. Zerwas, and P. M. Zerwas, Phys. Lett. B **707,** 512 (2012); B. Batell, S. Gori, and L.-T. Wang, J. High Energy Phys. 06 (2012) 172.

[26] A. Dedes, T. Figy, S. Hoche, F. Krauss, and T. E. J. Underwood, J. High Energy Phys. 11 (2008) 036.

[27] R. Barbieri, T. Gregoire, and L. J. Hall, arXiv:hep-ph/0509242.

[28] R. Foot, H. Lew, and R. R. Volkas, Phys. Lett. B **272,** 67 (1991); Mod. Phys. Lett. A **07,** 2567 (1992); S. Kanemura, S. Matsumoto, T. Nabeshima, and N. Okada, Phys. Rev. D **82,** 055026 (2010); O. Lebedev, H. M. Lee, and Y. Mambrini, Phys. Lett. B **707,** 570 (2012); L. Lopez-Honorez, T. Schwetz, and J. Zupan, Phys. Lett. B **716,** 179 (2012).

[29] S. Baek, P. Ko, and W.-I. Park, J. High Energy Phys. 02 (2012) 047; A. Djouadi, O. Lebedev, Y. Mambrini, and J. Quevillon, Phys. Lett. B **709,** 65 (2012); A. Djouadi, A. Falkowski, Y. Mambrini, and J. Quevillon, arXiv:1205.3169.

[30] M. Baak, M. Goebel, J. Haller, A. Hoecker, D. Kennedy, R. Kogler, K. Moenig, M. Schott, and J. Stelzer, Eur. Phys. J. C **72,** 2205 (2012).

[31] M. Bowen, Y. Cui, and J. D. Wells, J. High Energy Phys. 03 (2007) 036.

[32] O. J. P. Eboli and D. Zeppenfeld, Phys. Lett. B **495,** 147 (2000); Y. Bai, P. Draper, and J. Shelton, J. High Energy Phys. 07 (2012) 192; A. Djouadi, A. Falkowski, Y. Mambrini, and J. Quevillon, arXiv:1205.3169.

[33] M. Spira, A. Djouadi, D. Graudenz, and P. M. Zerwas, Nucl. Phys. **B453,** 17 (1995); M. Spira, Nucl. Instrum. Methods Phys. Res., Sect. A **389,** 357 (1997).

[34] T. Plehn, M. Spira, and P. M. Zerwas, Nucl. Phys. **B479,** 46 (1996); **B531,** 655(E) (1998); S. Dawson, S. Dittmaier and M. Spira, Phys. Rev. D **58,** 115012 (1998); see also M. Spira, HPAIR, http://people.web.psi.ch/spira/proglist.html.

[35] C. Englert, T. Plehn, D. Zerwas, and P. M. Zerwas, Phys. Lett. B **703,** 298 (2011).

[36] B. A. Dobrescu, G. D. Kribs, and A. Martin, Phys. Rev. D **85,** 074031 (2012); G. D. Kribs and A. Martin, Phys. Rev. D **86,** 095023 (2012).

[37] A. Arvanitaki, N. Craig, S. Dimopoulos, and G. Villadoro, arXiv:1210.0555; L. J. Hall, Y. Nomura, and S. Shirai, J. High Energy Phys. 01 (2013) 036.

[38] R. Barbieri, L. J. Hall, Y. Nomura, and V. S. Rychkov, Phys. Rev. D **75,** 035007 (2007); L. J. Hall, D. Pinner, and J. T. Ruderman, J. High Energy Phys. 04 (2012) 131.

[39] C. Csaki, C. Grojean, H. Murayama, L. Pilo, and J. Terning, Phys. Rev. D **69,** 055006 (2004); C. Csaki, C. Grojean, L. Pilo, and J. Terning, Phys. Rev. Lett. **92,** 101802 (2004).

[40] G. 't Hooft, Nucl. Phys. **B72,** 461 (1974); E. Witten, Nucl. Phys. **B160,** 57 (1979).

[41] N. Arkani-Hamed, M. Porrati, and L. Randall, J. High Energy Phys. 08 (2001) 017; R. Rattazzi and A. Zaffaroni, J. High Energy Phys. 04 (2001) 021.

[42] L. Randall and R. Sundrum, Phys. Rev. Lett. **83,** 3370 (1999); W. D. Goldberger and M. B. Wise, Phys. Rev. Lett. **83,** 4922 (1999); O. DeWolfe, D. Z. Freedman, S. S. Gubser, and A. Karch, Phys. Rev. D **62,** 046008 (2000).

[43] H. Georgi, D. B. Kaplan, and P. Galison, Phys. Lett. **143B,** 152 (1984).

[44] For review see, e.g., M. Perelstein, Prog. Part. Nucl. Phys. **58,** 247 (2007).

[45] R. Contino, Y. Nomura, and A. Pomarol, Nucl. Phys. **B671,** 148 (2003).

[46] G. F. Giudice, C. Grojean, A. Pomarol, and R. Rattazzi, J. High Energy Phys. 06 (2007) 045.

[47] G. Panico and A. Wulzer, J. High Energy Phys. 09 (2011) 135; J. Mrazek, A. Pomarol, R. Rattazzi, M. Redi, J. Serra, and A. Wulzer, Nucl. Phys. **B853,** 1 (2011).

[48] K. Cheung and T.-C. Yuan, Phys. Rev. Lett. **108,** 141602 (2012); Z. Chacko, R. Franceschini, and R. K. Mishra, arXiv:1209.3259; T. Abe, R. Kitano, Y. Konishi, K.-y. Oda, J. Sato, and S. Sugiyama, Phys. Rev. D **86,** 115016 (2012); B. Bellazzini, C. Csaki, J. Hubisz, J. Serra, and J. Terning, arXiv:1209.3299.

[49] S. Matsuzaki and K. Yamawaki, arXiv:1207.5911; Phys. Rev. D **86,** 115004 (2012); C. Coriano, L. D. Rose, C. Marzo, and M. Serino, Phys. Lett. B **717,** 182 (2012); J. Ellis, M. Karliner, and M. Praszalowicz, arXiv:1209.6430; B. A. Campbell, J. Ellis, and K. A. Olive, J. High Energy Phys. 03 (2012) 026.

[50] W. D. Goldberger, B. Grinstein, and W. Skiba, Phys. Rev. Lett. **100,** 111802 (2008).

[51] J. Fan, W. D. Goldberger, A. Ross, and W. Skiba, Phys. Rev. D **79,** 035017 (2009).

[52] B. A. Campbell, J. Ellis, and K. A. Olive, J. High Energy Phys. 03 (2012) 026.

[53] B. Coleppa, T. Gregoire, and H. E. Logan, Phys. Rev. D **85,** 055001 (2012).

[54] V. Barger, M. Ishida, and W.-Y. Keung, Phys. Rev. D **85,** 015024 (2012).

[55] A. V. Manohar and M. B. Wise, Phys. Lett. B **636,** 107 (2006).

[56] B. A. Kniehl and M. Spira, Z. Phys. C **69,** 77 (1995).

[57] J. Ellis, M. K. Gaillard, and D. V. Nanopoulos, Nucl. Phys. **B106,** 292 (1976); M. A. Shifman, A. I. Vainshtein, M. B. Voloshin, and V. I. Zakharov, Yad. Fiz. **30,** 1368 (1979) [Sov. J. Nucl. Phys. **30,** 711 (1979)].

[58] S. L. Adler, J. C. Collins, and A. Duncan, Phys. Rev. D **15,** 1712 (1977); Y. Iwasaki, Phys. Rev. D **15,** 1172 (1977).

[59] B. A. Dobrescu and J. D. Lykken, arXiv:1210.3342.

[60] A. De Roeck et al., Eur. Phys. J. C **66,** 525 (2010).

[61] Z. Komargodski and A. Schwimmer, J. High Energy Phys. 12 (2011) 099.

[62] Z. Komargodski, J. High Energy Phys. 07 (2012) 069.

[63] K. Agashe, R. Contino, and A. Pomarol, Nucl. Phys. **B719,** 165 (2005).

[64] S. R. Coleman and E. J. Weinberg, Phys. Rev. D **7,** 1888 (1973).

[65] K. Agashe and R. Contino, Nucl. Phys. **B742,** 59 (2006).

[66] R. Contino, L. Da Rold, and A. Pomarol, Phys. Rev. D **75,** 055014 (2007).

[67] Y. Hosotani, Phys. Lett. **129B,** 193 (1983); **126B,** 309 (1983); Ann. Phys. (N.Y.) **190,** 233 (1989).

[68] G. Panico, M. Redi, A. Tesi, and A. Wulzer, arXiv:1210.7114.

[69] R. Grober and M. Muhlleitner, J. High Energy Phys. 06 (2011) 020.

[70] R. Contino, M. Ghezzi, M. Moretti, G. Panico, F. Piccinini, and A. Wulzer, J. High Energy Phys. 08 (2012) 154.

[71] R. Contino, C. Grojean, M. Moretti, F. Piccinini, and R. Rattazzi, J. High Energy Phys. 05 (2010) 089.

[72] J. R. Espinosa, C. Grojean, and M. Muhlleitner, J. High Energy Phys. 05 (2010) 065.

[73] M. Gillioz, R. Grober, C. Grojean, M. Muhlleitner, and E. Salvioni, J. High Energy Phys. 10 (2012) 004.

[74] S. Dawson, E. Furlan, and I. Lewis, Phys. Rev. D **87,** 014007 (2013).

[75] T. Figy, Mod. Phys. Lett. A **23,** 1961 (2008).

[76] J. Bagger, V. D. Barger, K.-m. Cheung, J. F. Gunion, T. Han, G. A. Ladinsky, R. Rosenfeld, and C. P. Yuan, Phys. Rev. D **49,** 1246 (1994); J. Chang, K. Cheung, P.-Y. Tseng, and T.-C. Yuan, J. High Energy Phys. 12 (2012) 058; D. B. Franzosi and R. Foadi, arXiv:1209.5913.

[77] R. Contino, D. Marzocca, D. Pappadopulo, and R. Rattazzi, J. High Energy Phys. 10 (2011) 081.

[78] B. Bellazzini, C. Csaki, J. Hubisz, J. Serra, and J. Terning, J. High Energy Phys. 11 (2012) 003.

[79] E. Furlan, J. High Energy Phys. 10 (2011) 115.

[80] A. Pierce, J. Thaler, and L.-T. Wang, J. High Energy Phys. 05 (2007) 070; T. Corbett, O. J. P. Eboli, J. Gonzalez-Fraile, and M. C. Gonzalez-Garcia, Phys. Rev. D **86,** 075013 (2012); F. Bonnet, T. Ota, M. Rauch, and W. Winter, Phys. Rev. D **86,** 093014 (2012).

[81] M. E. Peskin and T. Takeuchi, Phys. Rev. D **46,** 381 (1992).

[82] J. Alcaraz et al. (ALEPH, DELPHI, L3, OPAL and LEP Electroweak Working Group Collaborations), arXiv:hep-ex/0612034.